Colloids and Surfaces B: Biointerfaces 122 (2014) 85–89

Colloids and Surfaces B: Biointerfaces

journal homepage: www.elsevier.com/locate/colsurfb

Enhanced laminin adsorption on nanowires compared to flat surfaces

Greger Hammarin[a,b], Henrik Persson[a,b], Aleksandra P. Dabkowska[b,c], Christelle N. Prinz[a,b,d,*]

[a] Division of Solid State Physics, Lund University, Lund, Sweden
[b] The Nanometer Structure Consortium, Lund University, Lund, Sweden
[c] Division of Physical Chemistry, Lund University, Lund, Sweden
[d] Neuronano Research Center, Lund University, Lund, Sweden

ARTICLE INFO

Article history:
Received 1 April 2014
Received in revised form 20 May 2014
Accepted 20 June 2014
Available online 28 June 2014

Keywords:
Laminin
Nanowires
Nanotopography
Cell adhesion
Protein
Curvature

ABSTRACT

Semiconductor nanowires are widely used to interface living cells, and numerous nanowire-based devices have been developed to manipulate or sense cell behavior. We have, however, little knowledge on the nature of the cell–nanowire interface. Laminin is an extracellular matrix protein promoting cell attachment and growth. Here, we used a method based on fluorescence microscopy and measured the relative amount of laminin adsorbed on nanowires compared to flat surfaces. The amount of adsorbed laminin per surface area is up to 4 times higher on 55 nm diameter gallium phosphide nanowires compared to the flat gallium phosphide surface between the nanowires. We show that this enhanced adsorption on nanowires cannot be attributed to electrostatic effects, nor to differences in surface chemistry, but possibly to pure geometrical effects, as increasing the nanowire diameter results in a decreased amount of adsorbed protein. The increased adsorption of laminin on nanowires may explain the exceptionally beneficial properties of nanowire substrates for cellular growth reported in the literature since laminin is often used as surface coating prior to cell cultures in order to promote cell growth, and also because primary cell suspensions contain endogenous laminin.

1. Introduction

Cell proliferation, morphology and adhesion on surfaces are strongly influenced by the topographical and chemical nature of the substrates. For instance, fibroblast spreading can be tuned by controlling the RGD (Arg-Gly-Asp) ligand density and clustering on the substrate [1,2]. There are three possible components in the cell response to different topographies: topography per se, biochemistry and substrate mechanical stiffness. Cells respond to the surface topography and one can find many examples in the literature of surfaces mimicking the extra-cellular matrix, which is not smooth and flat [3,4]. Cells are also sensitive to the stiffness of the substrate [5,6], which is directly influenced by the topography. For instance, a surface with long or low-density pillars will appear "softer" than a surface with shorter or denser pillars. Finally, cells are reacting to the biochemistry of the substrate, as mentioned above. In some cases, the topography and the biochemistry of the surface are linked. For instance, it has been shown that a specific nanotopography was adsorbing more fibronectin than other topographies, leading to the formation of more cell focal adhesion spots on this topography [7].

A few years ago, we showed that gallium phosphide (GaP) nanowires were excellent substrates for culturing neurons from the peripheral nervous system [8–10], which we recently confirmed applies for CNS neurons as well [11]. Since then, various studies have shown that different types of cells could be cultured on a wide range of nanowires [12–20]. We have shown that cell focal adhesions formed specifically on nanowires [21], suggesting a possible increase in molecules from the extracellular matrix (ECM), promoting cell adhesion and growth, on the nanowires. Among these ECM molecules, laminin is a 900 kDa extracellular protein that can bind to the cell transmembrane receptor integrins, and can trigger the formation of focal adhesions. Laminin is widely used for coating substrates before cell cultures, as it has been shown to increase cell adhesion and growth on the substrate [22,23].

Here, we used fluorescence microscopy to quantify the relative laminin adsorption on nanowires compared to flat surfaces. The laminin is adsorbed on vertical nanowire array substrates and is subsequently fluorescently labeled using immunochemistry. The

* Corresponding author at: Lund University, Division of Solid State Physics, Box 118, 221 00 Lund, Sweden. Tel.: +46 46 222 4796.
E-mail address: christelle.prinz@ftf.lth.se (C.N. Prinz).

http://dx.doi.org/10.1016/j.colsurfb.2014.06.048

amount of photons detected from the nanowires and from the flat surface are normalized to the surface area and compared. The effects of surface chemistry and nanowire diameter are investigated.

2. Materials and methods

2.1. Nanowires

Gallium phosphide nanowires were grown using metal organic vapor phase epitaxy (MOVPE) from catalytic gold nanoparticles [24]. Pure single crystalline gold nanoparticles with either 40 or 80 nm diameter were deposited randomly on a GaP (111)B substrate by aerosol deposition [25]. The average particle density on the surface was chosen to be 0.2, 0.5 or 1 μm^{-2}. The substrates were subsequently transferred to a commercial MOVPE reactor (Aixtron 200/4, Aixtron AG) for nanowire growth as previously described [26,27]. In order to remove the surface oxide and to alloy the Au particles with the substrate, the samples were annealed at 470 °C for 10 min in an atmosphere of hydrogen and phosphine. The nanowire growth was conducted at low pressure (10 kPa) and was initiated by supplying trimethylgallium in addition to the phosphine at 470 °C. The nanowire length was controlled by adjusting the duration of the growth and was chosen to be between 2 and 5 μm, depending on the sample. The nanowire diameter was determined by the gold particle size and was typically 55 nm and 90 nm for a nominal 40 nm and 80 nm diameter Au nanoparticle, respectively. The resulting GaP nanowires were perpendicular to the surface with very low tapering and with exceptional homogeneity in the dimensions of the nanowires. Some nanowire substrates were sputtered with SiO_x (AJA Orion 5 sputtering system) in order to cover the GaP material, as well as to increase the nanowire diameter to larger diameters, usually not achievable using our aerosol set-up.

2.2. Determination of the nanowire dimensions

The nanowire substrates were characterized using scanning electron microscopy (SEM), in a FEI NanoLab 600 FIB/SEM system. The lengths of the nanowires were measured and the nanowire diameters were measured at mid length. The measurements were repeated for 10 nanowires at each of five different places of the approximately 20 mm^2 large samples. The diameter variation within a given sample was ±5 nm and the length variation was ±0.2 μm. In the case of SiO_x-sputtered nanowires, the final diameter variation was ±10 nm.

2.3. Laminin adsorption

A solution of laminin from Engelbreth–Holm–Swarm murine sarcoma basement membrane at 1 mg/mL in Tris buffered NaCl (Sigma Aldrich) was thawed on ice and diluted to a final concentration of 0.1 μg/mL in either RPMI 1640 culture medium (Sigma Aldrich) or in phosphate buffer saline (PBS). A 2 mL volume of the 0.1 μg/mL laminin solution was poured in a petri dish containing the nanowire substrate and incubated at room temperature for 1 h. Initially, the samples were then fixed in Stefanini fixative for 10 min before being rinsed 3 times in PBS. We later found out that the fixation step was not necessary and that the adsorbed laminin ratio was the same (and stable for days), when fixation was omitted. Therefore most of the samples were simply rinsed in PBS after laminin incubation.

2.4. Laminin immunostaining

The substrates were incubated in a 1:200 rabbit-anti-laminin IgG (Sigma Aldrich) in PBS containing 0.25% Triton X100 and 0.25% BSA for 2 h at room temperature. After rinsing seven times in PBS, the samples were incubated with 1:200 goat-anti rabbit-Alexa Fluor 488 IgG (Invitrogen) in PBS containing 0.25% triton X100 and 0.25% BSA for 2 h at room temperature, in the dark. The samples were subsequently rinsed several times in PBS. Nanowire substrates showed no detectable fluorescence when no primary antibodies were used or when no laminin was pre-adsorbed on the sample.

2.5. Direct laminin labeling with Alexa Fluor 488

We labeled laminin directly with Alexa Fluor 488 using the Alexa-Fluor 488 protein labeling kit (Invitrogen). Briefly, the Tris buffered NaCl solvent of the 1 mg/mL laminin stock solution was exchanged for PBS using a NAP-5 column (GE Healthcare Life Sciences) before using the protein labeling kit. The method is optimized for labeling small IgG proteins: even though we could collect a band of fluorescently labeled proteins, the concentration could not be determined using a spectrophotometer (Nanodrop), implying that it was below the 0.1 mg/mL detection limit. The labeled laminin solution was diluted 40 times in PBS before being poured on the GaP nanowire substrates for a one-hour incubation time in the dark, at room temperature. The samples were then rinsed in PBS.

2.6. Confocal microscopy

The samples were imaged using a Zeiss LSM 510 confocal microscope with a 63× oil immersion objective (1.4 N.A.). The optical slice was set to the maximum, corresponding to 7.3 μm. The optical slice should be larger than the nanowire length in order to collect the fluorescence from the laminin adsorbed on both the nanowires and the surface in the same image. The gain was adjusted to the highest value for which no pixels would be saturated. Line-averaged 4 times, 2048 × 2048 pixel images were taken for all samples at a 1× magnification in the LSM software, corresponding to a 142.86^2 μm^2 area.

The linearity of the response of the photodetectors was verified by using a concentration series of the ATTO488 dye (Sigma Aldrich) in water (Excitation 488 nm, Emission 523 nm). Confocal z-stack images of the nanowire arrays were also acquired. In this case, the optical slice was chosen to be 0.8 μm and the increment between two consecutive stack images was 0.4 μm. The corresponding 3 dimensional image was then generated using the ImageJ software (version 1.44, National Institute of Health, USA).

2.7. Analysis

The confocal images were analyzed using ImageJ. On single-plane images (as shown in Fig. 2b for instance), a rectangular area was chosen, typically containing tens of nanowires. The total number of pixels (P), as well as the mean counts per pixel (Mean C) was extracted. The exact number of nanowires (N) in the selected square was counted. A smaller square containing no nanowires was then selected, and the mean count (Mean C surface) was extracted from the image.

The number of counts per surface area (μm^{-2}) on the nanowires was calculated as:

$$\mathrm{NW} = \frac{P(\mathrm{Mean}\,C - \mathrm{Mean}\,C\ \mathrm{surface})}{N\pi DL} \pm \Delta(\mathrm{NW})$$

where D is the nanowire diameter and L is the nanowire length.

The uncertainty is estimated to be:

$$\Delta\mathrm{NW} = \left(\frac{\Delta(\mathrm{Mean}\,C\ \mathrm{surface})}{\mathrm{Mean}\,C\ \mathrm{surface}} + \frac{\Delta(D)}{D} + \frac{\Delta(L)}{L}\right)\mathrm{NW}$$

where $\Delta(D) = 5$ nm and $\Delta(L) = 0.2$ μm.

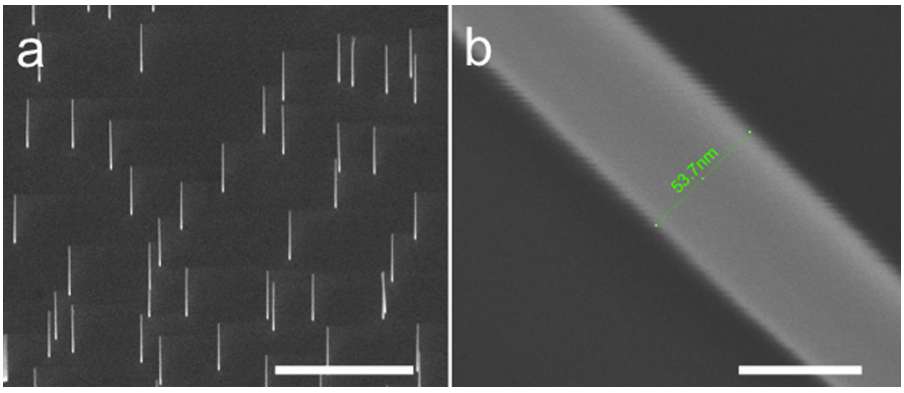

Fig. 1. Example of vertical nanowire array used in this study. (a) Scanning electron microscope image of 55 nm diameter, 5 μm long, vertical gallium phosphide nanowires. Tilt 20°, scale bar 5 μm. (b) Scanning electron microscope close up image of a 55 nm diameter nanowire. Scale bar 50 nm.

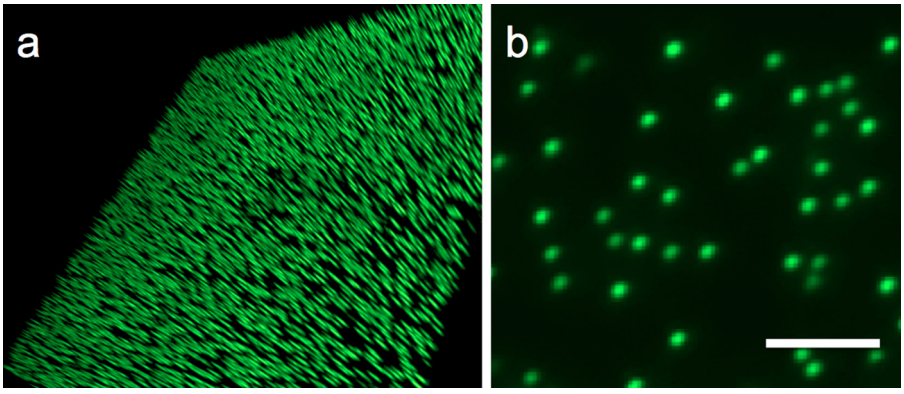

Fig. 2. Laminin adsorbed on a GaP nanowire substrate. Confocal 3-dimensional stack image of a 143 × 143 μm² area with vertical 90 nm diameter, 3.2 μm long GaP nanowires (a). Single plane image (7.3 μm optical slice) of the same sample (b). Scale bar 3 μm.

The number of counts per surface area (μm^{-2}) on the surface was calculated as:

$$\text{Surface} = \frac{\text{Mean } C \text{ surface} \times 2048^2}{142.86^2} \pm \Delta(\text{Surface})$$

where

$$\Delta(\text{Surface}) = \frac{\Delta\text{Mean } C \text{ surface} \times 2048^2}{142.86^2}$$

Finally, the relative laminin adsorption on the nanowires was calculated as:

$$\text{Relative laminin adsorption} = \frac{\text{NW}}{\text{Surface}} \pm \left(\frac{\Delta(\text{NW})}{\text{NW}} + \frac{\Delta(\text{Surface})}{\text{Surface}} \right) \frac{\text{Surface}}{\text{NW}}$$

The different sets of data were compared using the Wilcoxon–Mann–Whitney test in Kaleidagraph (Synergy software).

3. Results and discussion

Substrates with nanowires of 55 nm in diameter and nanowires of 90 nm (Fig. 1) in diameter were incubated with laminin, which was subsequently stained using polyclonal primary antibodies and Alexa Fluor 488-conjugated secondary antibodies.

Fig. 2 shows a z-stack confocal image and a single 7.3 μm-thick planar image of the nanowire substrate with adsorbed immunostained laminin. The fluorescence is much stronger on the nanowires than on the flat substrate. Vertical nanowire arrays have recently been proposed as tools for protein detection, isolation and analysis because of the increased surface area they provide [28,29]. In order to test whether the increase in fluorescence on the nanowire was due to the increased surface area alone, we normalized the fluorescence to the surface area (see experimental section for detailed analysis protocol).

When normalized to the surface area, we observed a higher amount of laminin adsorbed on the nanowires compared to the flat surface (Fig. 3). The data shows that 4 times the amount of laminin adsorbs to 55 nm diameter nanowires compared to the flat surface and more than double the amount of laminin adsorbs to 90 nm diameter nanowires compared to the flat surface. Fluorescence images of nanowires lying horizontally on the substrates showed a homogeneous fluorescence intensity along the length of the nanowires (see Supplementary Figure 1), ruling out any possible metal enhanced fluorescence phenomenon due to the presence of a gold nanoparticle at the tip of the nanowire.

Several groups have reported a strong influence of nanoparticle curvature on the adsorbed protein amount and conformation [30–32], as well as a higher protein adsorption on nano-structured substrates compared to flat surfaces [7,33–35]. In the case of laminin, it has been suggested that the conformation of laminin on nano-islands was different than the one on flat substrates and resulted in more antibody binding sites being available [30].

In order to test whether this could also be the case of laminin adsorbed on nanowires, we labeled laminin directly with the fluorescent dye Alexa Fluor 488 nm before letting the protein adsorb onto the nanowire substrate. We could not find any significant difference in the relative amount between pre-labeled laminin and laminin labeled using antibodies after adsorption (Fig. 4). This

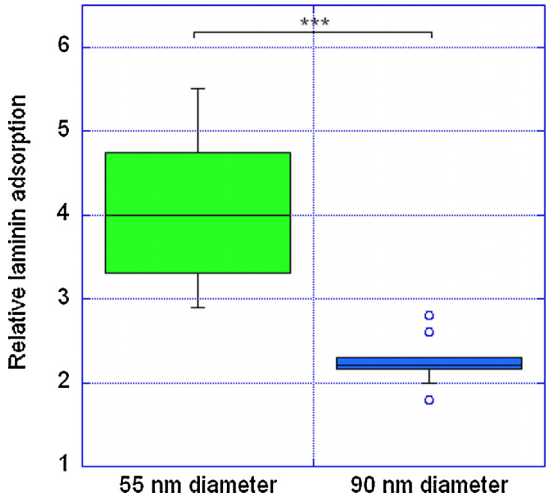

Fig. 3. Relative amount of laminin adsorbed on nanowires compared to the flat surface for nanowire diameters of 55 and 90 nm (median and four quartiles). $^{***}p < 0.001$ (Wilcoxon–Mann–Whitney test). Circles represent outliers.

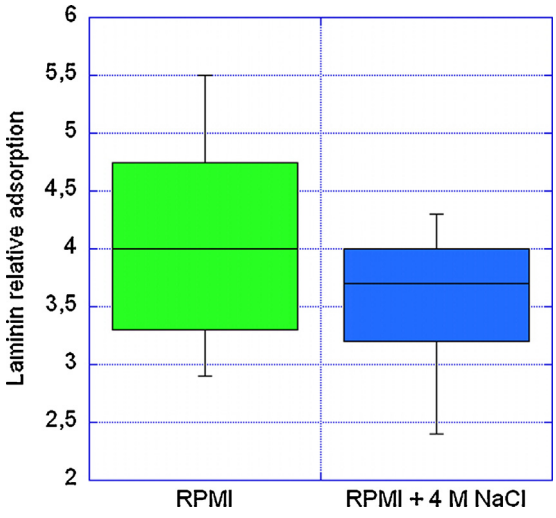

Fig. 5. Relative laminin adsorption on 55 nm GaP nanowires in cell culture medium (left) and relative laminin adsorption on 55 nm GaP nanowires in cell culture medium with 4 M added NaCl (right). We could not find any significant difference in laminin adsorption between both cases ($p = 0.23$, Wilcoxon–Mann–Whitney Test).

suggests that laminin on nanowires does not have more available binding sites compared to laminin on flat surfaces and shows that the observed enhancement in adsorbed laminin on nanowires is not an artifact of the protein labeling method used.

We tested whether the laminin adsorption could be attributed to electrostatic interactions and measured the relative amount of adsorbed laminin on 55 nm diameter nanowire in the presence of 4 M NaCl added in the cell culture medium. At this ionic strength, the Debye screening length κ^{-1} (at which the electrostatic interaction are screened) is 0.152 nm ($\kappa^{-1} = 0.304/\sqrt{[\mathrm{NaCl}]\,\mathrm{nm}}$) [36], which is very small compared to the size of a protein (10 nm for a standard protein, 50–100 nm for laminin). We can therefore conclude that there are no electrostatic interactions at this salt concentration. The enhanced adsorption of laminin on nanowires still takes place at 4 M NaCl (Fig. 5), which demonstrates that this phenomenom cannot be attributed to electrostatic interactions.

Comparing the relative amount of laminin on 55 and 90 nm diameter nanowires also shows an effect of the nanowire diameter (Fig. 3). In order to further test this effect, we sputtered nanowires with SiO_x and obtained nanowires with a uniform surface chemistry and final diameters of 78 nm, 130 nm and 260 nm. The relative laminin adsorption decreases with increasing nanowire diameter (Fig. 6). Laminin does not adsorb more on the 260 nm diameter nanowires compared to the flat surface. Our results thus suggest that laminin adsorption increases with the substrate curvature. This contrasts with the results of a recent study on nanobead arrays, showing a lower laminin adsorption on beads of higher curvature [32]. In our case, nanowires are several microns in length and are spaced several microns apart, which ensures that laminin molecules adsorbed on distinct nanowires do not interact with each other. On the other hand, in the study of the bead substrate ([32]), the distance between beads was on the same order of magnitude as the radius of gyration of laminin, a distance at which one can expect steric interactions between proteins adsorbed on neighboring beads resulting in a lower protein adsorption. The fact that SiO_x-coated nanowires have a uniform surface chemistry also rules out any possible effects from the GaP nanowire-wall crystalline

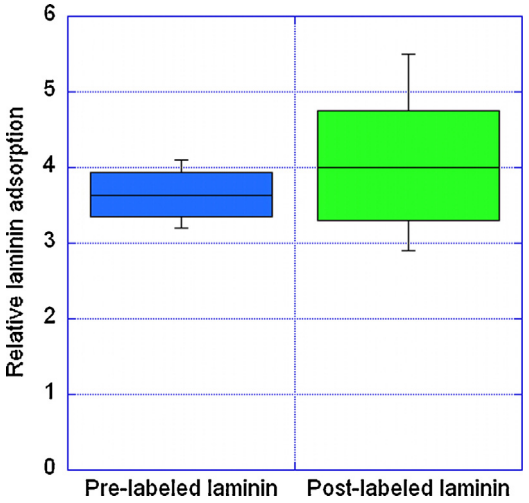

Fig. 4. Relative adsorption of laminin on nanowires. Prelabeled laminin refers to laminin labeled using the Alexa-Fluor Protein labeling kit before adsorption on the nanowires (diameter 50 nm). Post-labeled laminin refers to laminin stained using primary antibodies and secondary Alexa Fluor conjugated antibodies after adsorption on the nanowires (diameter 55 nm). We could not find any significant difference in laminin adsorption between both cases ($p = 0.55$, Wilcoxon–Mann–Whitney Test).

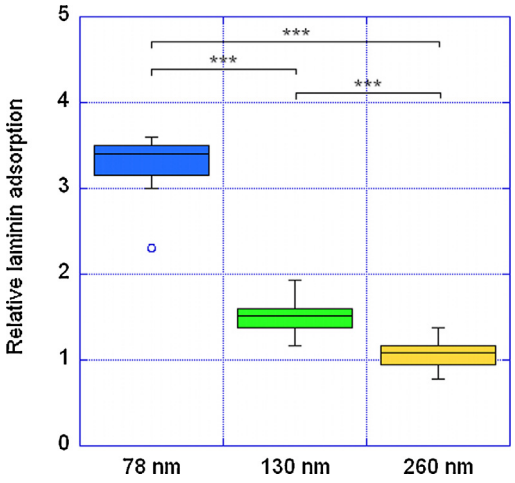

Fig. 6. Relative adsorption of laminin for SiO_x sputtered GaP nanowires of 78 nm, 130 nm and 260 nm final diameter (median and four quartiles). $^{***}p < 0.001$ (Wilcoxon–Mann–Whitney test). Circles represent outliers.

planes, which differ from GaP (111)B, or from possible dangling bonds, in the observed enhanced laminin adsorption.

Using the sodium dodecyl sulfate polyacrylamide gel electrophoresis (SDS-PAGE) method as an alternative method to measure the amount of laminin adsorbed to nanowires, we were not able to detect any laminin. This is most probably due to an insufficient amount of proteins, which is a direct result of the low number of nanowires available. In contrast, the fluorescence method presented here requires only a few mm^2 for each sample and might be used for other nanoparticles that are too expensive to produce in big quantities.

4. Conclusions

We have used a fluorescence microscopy method to measure the relative amount of laminin adsorbed on GaP nanowires compared to flat GaP surface. Laminin adsorbs up to 4 times more on 55 nm diameter nanowires, when normalized to the surface area, compared to the flat surface. We showed that this phenomenon is neither due to electrostatic effects, nor crystalline effects but may be attributed to purely geometric effects, with small-diameter nanowires having more adsorbed laminin per surface area compared to nanowires with larger diameters. Preferential adsorption of the ECM protein laminin to nanowires may be part of the explanation why nanowire substrates are beneficial for cell attachment and growth.

Acknowledgements

The authors would like to thank Gaëlle Piret and Martina Schneider for help with the spectrophotometer and Tommy Cedervall for help with the polyacrylamide gels. This work was performed at the Microscopy Facility at the Department of Biology, Lund University. This work was funded by the Swedish research council (VR) and the Nanometer Structure Consortium at Lund University (nmC@LU).

Appendix A. Supplementary data

Supplementary material related to this article can be found, in the online version, at http://dx.doi.org/10.1016/j.colsurfb.2014.06.048.

References

[1] E.A. Cavalcanti-Adam, T. Volberg, A. Micoulet, H. Kessler, B. Geiger, J.P. Spatz, Biophys. J. 92 (2007) 2964.
[2] M. Schvartzman, M. Palma, J. Sable, J. Abramson, X.A. Hu, M.P. Sheetz, S.J. Wind, Nano Lett. 11 (2011) 1306.
[3] R.G. Flemming, C.J. Murphy, G.A. Abrams, S.L. Goodman, P.F. Nealey, Biomaterials 20 (1999) 573.
[4] M. Lai, K. Cai, Y. Hu, X. Yang, Q. Liu, Colloids Surf. B Biointerf. 97 (2012) 211.
[5] D.E. Discher, P. Janmey, Y. Wang, Science 310 (2005) 1139.
[6] M. Ghibaudo, A. Saez, L. Trichet, A. Xayaphoummine, J. Browaeys, P. Silberzan, A. Buguin, B. Ladoux, Soft Matter 4 (2008) 1836.
[7] A. Dolatshahi-Pirouz, T. Jensen, D.C. Kraft, M. Foss, P. Kingshott, J.L. Hansen, A.N. Larsen, J. Chevallier, F. Besenbacher, ACS Nano 4 (2010) 2874.
[8] W. Hallstrom, T. Martensson, C. Prinz, P. Gustavsson, L. Montelius, L. Samuelson, M. Kanje, Nano Lett. 7 (2007) 2960.
[9] W. Hällström, C.N. Prinz, D. Suyatin, L. Samuelson, L. Montelius, M. Kanje, Langmuir 25 (2009) 4343.
[10] W. Hällström, M. Lexholm, D.B. Suyatin, G. Hammarin, D. Hessman, L. Samuelson, L. Montelius, M. Kanje, C.N. Prinz, Nano Lett. 10 (2010) 782.
[11] G. Piret, M.-T. Perez, C.N. Prinz, Biomaterials 34 (2013) 875.
[12] K. Adolfsson, H. Persson, J. Wallentin, S. Oredsson, L. Samuelson, J.O. Tegenfeldt, M.T. Borgstrom, C.N. Prinz, Nano Lett. 13 (2013) 4728.
[13] T. Berthing, S. Bonde, C.B. Sorensen, P. Utko, J. Nygard, K.L. Martinez, Small 7 (2011) 640.
[14] L. Hanson, Z.C. Lin, C. Xie, Y. Cui, B.X. Cui, Nano Lett. 12 (2012) 5815.
[15] W. Kim, J.K. Ng, M.E. Kunitake, B.R. Conklin, P.D. Yang, J. Am. Chem. Soc. 129 (2007) 7228.
[16] F. Mumm, K.M. Beckwith, S. Bonde, K.L. Martinez, P. Sikorski, Small 9 (2013) 263.
[17] H. Persson, J.P. Beech, L. Samuelson, S. Oredsson, C.N. Prinz, J.O. Tegenfeldt, Nano Res. 5 (2012) 190.
[18] H. Persson, C. Købler, K. Mølhave, L. Samuelson, J.O. Tegenfeldt, S. Oredsson, C.N. Prinz, Small 9 (2013) 4006.
[19] A.K. Shalek, J.T. Robinson, E.S. Karp, J.S. Lee, D.-R. Ahn, M.-H. Yoon, A. Sutton, M. Jorgolli, R.S. Gertner, T.S. Gujral, G. MacBeath, E.G. Yang, H. Park, Proc. Natl. Acad. Sci. U.S.A. 107 (2010) 1870.
[20] C. Xie, L. Hanson, W.J. Xie, Z.L. Lin, B.X. Cui, Y. Cui, Nano Lett. 10 (2010) 4020.
[21] C. Prinz, W. Hallstrom, T. Martensson, L. Samuelson, L. Montelius, M. Kanje, Nanotechnology 19 (2008) 345101.
[22] A. Vallee, M.G. Faga, F. Mussano, F. Catalano, E. Tolosano, S. Carossa, F. Altruda, G. Martra, Colloids Surf. B Biointerf. 114 (2014) 284.
[23] K. Cai, H. Dong, C. Chen, L. Yang, K.D. Jandt, L. Deng, Colloids Surf. B Biointerf. 72 (2009) 230.
[24] W. Seifert, M. Borgstrom, K. Deppert, K.A. Dick, J. Johansson, M.W. Larsson, T. Martensson, N. Sköld, C.P.T. Svensson, B.A. Wacaser, L.R. Wallenberg, L. Samuelson, J. Cryst. Growth 272 (2004) 211.
[25] M.H. Magnusson, K. Deppert, J.-O. Malm, J.-O. Bovin, L. Samuelson, Nanostructured Mater 12 (1999) 45.
[26] D.B. Suyatin, W. Hallstram, L. Samuelson, L. Montelius, C.N. Prinz, M. Kanje, J. Vac. Sci. Technol. B 27 (2009) 3092.
[27] C.E. Linsmeier, C.N. Prinz, L.M.E. Pettersson, P. Caroff, L. Samuelson, J. Schouenborg, L. Montelius, N. Danielsen, Nano Lett. 9 (2009) 4184.
[28] V. Krivitsky, L.C. Hsiung, A. Lichtenstein, B. Brudnik, R. Kantaev, R. Elnathan, A. Pevzner, A. Khatchtourints, F. Patolsky, Nano Lett. 12 (2012) 4748.
[29] K.R. Rostgaard, R.S. Frederiksen, Y.C. Liu, T. Berthing, M.H. Madsen, J. Holm, J. Nygard, K.L. Martinez, Nanoscale 5 (2013) 10226.
[30] P. Roach, D. Farrar, C.C. Perry, J. Am. Chem. Soc. 128 (2006) 3939.
[31] M. Lundqvist, I. Sethson, B.H. Jonsson, Langmuir 20 (2004) 10639.
[32] A.A. Vertegel, R.W. Siegel, J.S. Dordick, Langmuir 20 (2004) 6800.
[33] H. Agheli, J. Malmstrom, E.M. Larsson, M. Textor, D.S. Sutherland, Nano Lett. 6 (2006) 1165.
[34] J. Malmstrom, H. Agheli, P. Kingshott, D.S. Sutherland, Langmuir 23 (2007) 9760.
[35] N. Giamblanco, E. Martines, G. Marletta, Langmuir 29 (2013) 8335.
[36] J.N. Israelachvili, Intermolecular and Surface Forces, Academic Press, London, 1992, chapter 12.